Bulletin of the Geological Survey of Japan, vol.31(10), p. 467–487, 1980 551.243.1

Magnitude-Frequency Relation for Displacement of Minor Faults and Its Significance in Crustal Deformation

Toshihiro KAKIMI*

KAKIMI, T. (1980) Magnitude-frequency relation for displacement of minor faults and its significance in crustal deformation. *Bull. Geol. Surv. Japan*, vol. 31(10), p. 467–487.

Abstract: Magnitude-frequency relation for the displacement of minor faults is examined in several cases in which the faulting conditions, such as stress state, sense of fault-slip, ductility of materials etc., are different from each other. In every case the number N of the faults with throw between T and $T + dT$ is expressed approximately as $N(T)dT = KT^{-m}dT$, or, $\log N(T) = k - m \log T$, where K, k and m are the numerical constants. Values m fall into a wide range of 1.3 to 2.4 for minor faults developed in the Neogene strata of the South Kanto district.

The coefficients K and k are the function of area and density of fault displacement related to the intensity of regional deformation. The exponent m indicates the spectral structure on the magnitude of fault displacement related actually to the tectonic conditions in the faulted region, such as the homogeneity of mechanical structure, stability of stress field, sharpness of regional deformation, etc.. The variation in m-values obtained is likely to refrect well the differences in tectonic conditions in the observed region.

Since the throw in each fault is a result of repeated slips, N-T relation may vary with time corresponding to the degree of progressive deformation. In the earlier stage of faulting, m will be large in value for both sets of a conjugate fault system. In the more matured stage, either one of the two sets will become predominant so that its m-value will decrease, whereas m of the other set will remain at the earlier stage. Thus, the magnitude-frequency relation for fault displacement expressed by the above equations is useful for estimating the regional and temporal variations in tectonic conditions.

1. Introduction

Minor faults whose displacement is mesoscopic in scale, on the order of millimeters to a few meters, have long been investigated in detail mainly in order to ascertain the *stress field* and *tectonic conditions* such as strength of materials, ductility, depth from the ground surface, etc., under which these faults were generated. On the other hand, quantitative studies on *strain distribution* using minor faults have been scracely found in spite of their importance as well. Minor faults tend to be thought that they are of minor contribution for regional deformation of rocks as compared with "major faults" which have been considered to bear the "major" portion of deformation, even if they are few in number. However, since the minor faults are much abundant in number than the major faults, accumulated amount of displacement by the minor faults should never be negligible as compared with that by the major faults.

In this viewpoint, the present writer and his collaborator (KAKIMI and KODAMA, 1974) treated statistically the distribution (spectrum) of displacement in minor faults having normal-slip sense observed in a certain area, and proposed, as a first approximation, following formulae for representing the frequency of faults as a function of their displacement;

$$N(T)dT = KT^{-m}dT, \quad (1)$$

or

$$\log N(T) = k - m \log T. \quad (2)$$

* Environmental Geology Department

In these equations the number of faults with displacement (downthrow, in this case) between T and $T + dT$ is denoted by $N(T)dT$, while K, k ($= \log K$) and m are constants. They pointed out that Eq. (1) takes the same form with the well-known Ishimoto-Iida's (1939) formula expressing the frequency distribution of earthquakes in respect to maximum trace amplitude a recorded at a certain station, by

$$n(a)da = ka^{-m}da, \qquad (3)$$

where $n(a)da$ is the number of earthquakes having a maximum trace amplitude a to $a + da$, and k and m are both constants. Ishimoto-Iida's formula is closely related to Gutenberg-Richter's formula, the most widely used one for representing the magnitude-frequency relation of earthquakes expressed at first by GUTENBERG and RICHTER (1944) as

$$\log n(M) = a - bM. \qquad (4)$$

In this equation the number of earthquakes with magnitude between M and $M + dM$ is denoted by $n(M)dM$ and a and b are both constants. Under some reasonable assumptions (ASADA *et al.*, 1951), Eq. (3) is equivalent to Eq. (4) in which the coefficient b is connected with the exponent m by the equation

$$m = b + 1. \qquad (5)$$

The physical meanings of these formulae and of the exponent m and coefficient b were discussed by MOGI (1962) based upon the results of laboratory experiments on the fracturing of various materials. In his papers it was deduced that the magnitude (amplitude)-frequency relation of elastic shocks accompanying brittle fractures of heterogeneous materials depends both on the structural states of materials and the stress states in the medium, and that the exponent m increases with the degree of heterogeneity and that of the spatial variation in the stress distribution.

NAGUMO (1969) discussed the physical meanings of Ishimoto-Iida's formula (Eq. 3) from the viewpoint of theoretical relation between deformation and fracture. He pointed out, under some reasonable assumptions, that the power function representation of Ishimoto-Iida's formula is due to the same representation for the spectrum of plastic deformation of the medium, and the exponent m indicates the sharpness of the spectrum of the deformation.

In the previous paper (KAKIMI and KODAMA, 1974) a field example on magnitude-frequency relation of fracturing was first exhibited. However, the relation was examined only on a specified field and, therefore, discussions on the significance of Eq. (1) stayed in the preliminary state. In the present paper the magnitude-frequency relation of faulting is examined on various types of minor faults including those treated in the previous paper. Then, it is shown in this paper that Eq. (1) is a common formula expressing the strain distribution in a faulted area. The significance of the exponent m against the fracturing and deformation of an area are also dealt with.

2. Geologic and Tectonic Frameworks and General Aspect of Minor Faults Used for Analysis

Minor faults which the writer treated in the present paper are those developed in Miura and Boso Peninsulas, South Kanto district. General geology and geologic structures of the field are shown schematically in Fig. 1.

The Upper Miocene Miura Group, probably including the Lower Pliocene strata, is mainly composed of siltstone, sandstone and the alternation of them which are intercalated with thin layers of tuff. The uppermost part of the Group is composed of medium- to very coarse-grained sandstone of volcaniclastic materials such as pumice, scoria, lithic fragment, etc.

The Kazusa Group, Late Pliocene to Early Pleistocene in age, overlies the Miura Group with slightly oblique unconformity which are well known as the Kurotaki Unconformity. The Group is composed of volcaniclastic rocks in the basal part and of siltstone, sandy mudstone, well-sorted sandstone and the alternation of them in the main part. Thin tuff layers are also intercalated in the Group.

In both Groups siltstone and sandy mudstone

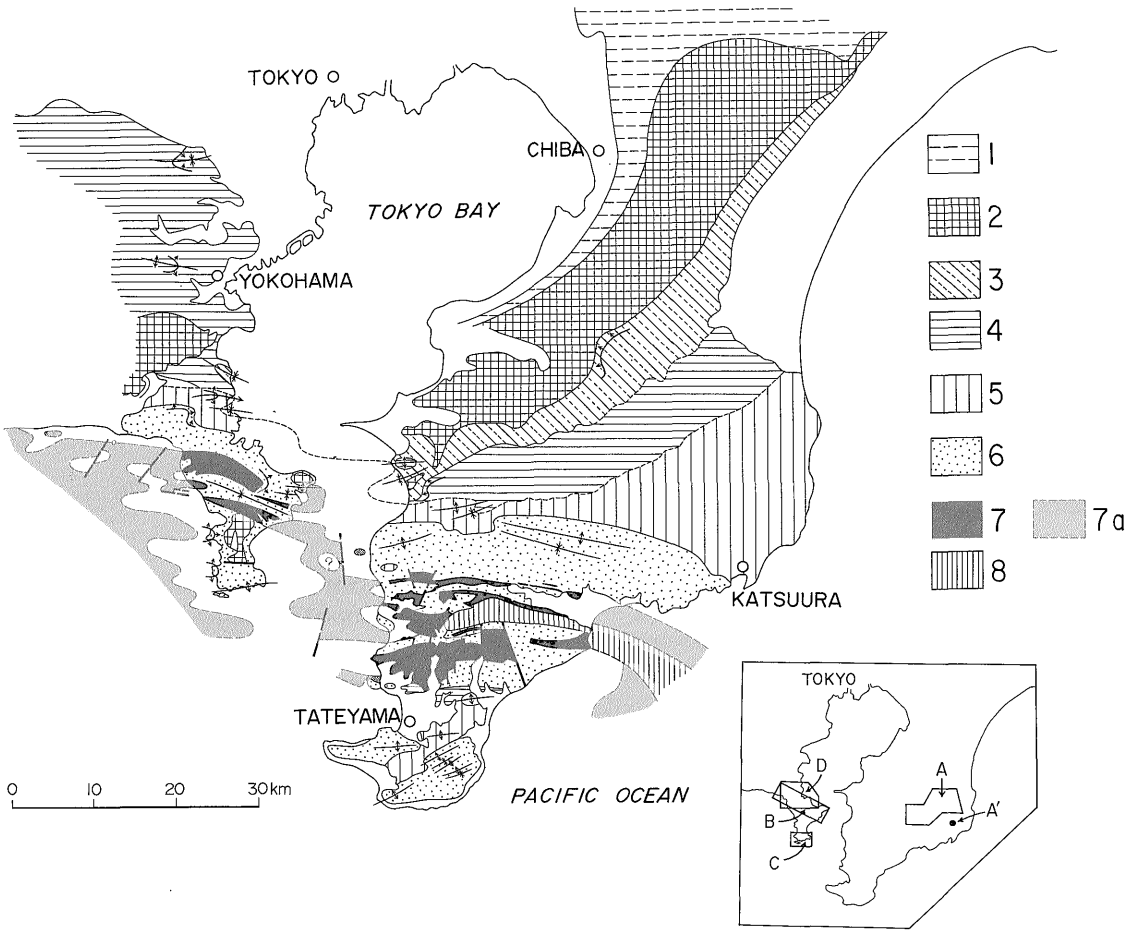

Fig. 1 Geological and tectonic sketch map of the South Kanto District (after MITSUNASHI, 1968).
1. Shimosueyoshi and Narita Formations, 2. Sagami Group, 3. Upper Kazusa Group, 4. Middle Kazusa Group, 5. Lower Kazusa Group, 6. Miura Group, 7. Hota Group, 7a. Hota Group in subsea areas, 8. Mineoka Group.
Insert is an index map in which A, B, C and D denote areas treated in the present paper as CASE-A, -B, -C and -D respectively. A′ denote the site near Onjuku where the fault density was examined.

are moderately consolidated while well-sorted sandstone is scarcely consolidated.

The structural trend of the upper Neogene and lower Pleistocene in the area is generally E–W as shown in Fig. 1. In this area, minor faults are developed as well as the faults of larger displacement. They are classified into several (six or more) fault systems on the basis of parallelism of fault-plane direction, mode of occurrence, successive relationship, etc. Using these fault systems the writer (KAKIMI, 1974) had clarified the temporal change in tectonic stress field since the latest Neogene to Quaternary in the area. Of these faults, those belonging among two systems, one of which is the Younger Normal-Fault System and the other is the Older Reverse-Fault System, both named by KAKIMI *et al.* (1966), are most widely and commonly found over both Peninsulas.

Faults of the Younger Normal-Fault System,

which the writer call hereafter the Younger Normal Faults, have strikes of approximate N–S and dip steeply toward E or W. It is considered from the conjugate relation of these faults that they were formed under a stress field where the axis of maximum tension lies nearly horizontal but dips gently toward E or W in locally. Small shear angle, 30° to 50° in general, and open slip-plane of these faults suggest that they had occurred under a brittle condition, probably at shallow subsurface depth.

Faults of the Older Reverse-Fault System, called here the Older Reverse Faults, have general strikes of E–W or WNW–ESE and slip-planes showing reverse separation. The fault surfaces are closed and lithified to the same degree as the surrounding rocks. When these faults are found in conjugate relation, shear angles are very large, sometimes exceeding 90 degrees. Fault drags are observed occasionally. All these characteristics suggest that the Older Reverse Faults had occurred under more ductile conditions than those under which the Younger Normal Faults were generated.

The Older Reverse Faults which are inferred to be generated during the Late Pliocene and Early Pleistocene are always cut off by the Younger Normal Faults generated probably during the Middle Pleistocene.

Fault examples which are treated for analysis in this paper belong either of two systems mentioned above as follows:

CASE-A: Younger Normal Faults in the eastern part of Boso Peninsula.

CASE-B: Younger Normal Faults in the northern part of Miura Peninsula.

CASE-C: Younger Normal Faults at the southern tip of Miura Peninsula.

CASE-D: Older Reverse Faults in the northern part of Miura Peninsula.

In every case treated here, the fault data were collected in former times by various investigators including the present writer mainly for the purpose of obtaining the information on stress conditions but not strain conditions. Therefore, as to the amounts of displacement, the collected data are not always strictly statistic (uniformly random). Especially on the range of fault-displacement less than ten centimeters the sampling number may be insufficient statistically as compared with the number of faults with larger displacement. A more correct (statistic) sampling was once carried out at a small area, as will be shown in the following section.

3. Frequency Distributions of Faults in Respect to Throw in the Several Cases

1) CASE-A: Younger Normal Faults in the eastern part of Boso Peninsula

The Younger Normal Faults which are predominantly developed in this area were investigated in detail by KINUGASA *et al.* (1969) at the coastal district and by the Minor Fault Research Group (MFRG, 1973) at the district around Otaki Town. From the conjugate relation of faulting, it is known that these faults are almost purely of normal-slip type having scarcely the strike-slip component.

In addition to the minor faults, the "major faults" of normal-slip sense whose range of displacement is from several meters to a hundred meters are well developed in the present area. They are represented well in precise geological maps prepared by KOIKE (1955), MITSUNASHI *et al.* (1961) and ISHIWADA *et al.* (1971) and are schematically shown in Fig. 2. From the parallelism of the fault-plane direction and the similarity of fault occurrences, the major and minor faults are considered to be formed together under the same stress field. Of these major faults arranged in conjugate relationship, the faults which dip toward east tend to develop more frequently than those dipping toward west, and therefore this area is subsided gradually eastwards as shown in Fig. 3.

Using the data on downthrow[1] of the minor

[1] Vertical component of normal separation is conventionally called downthrow in this paper.

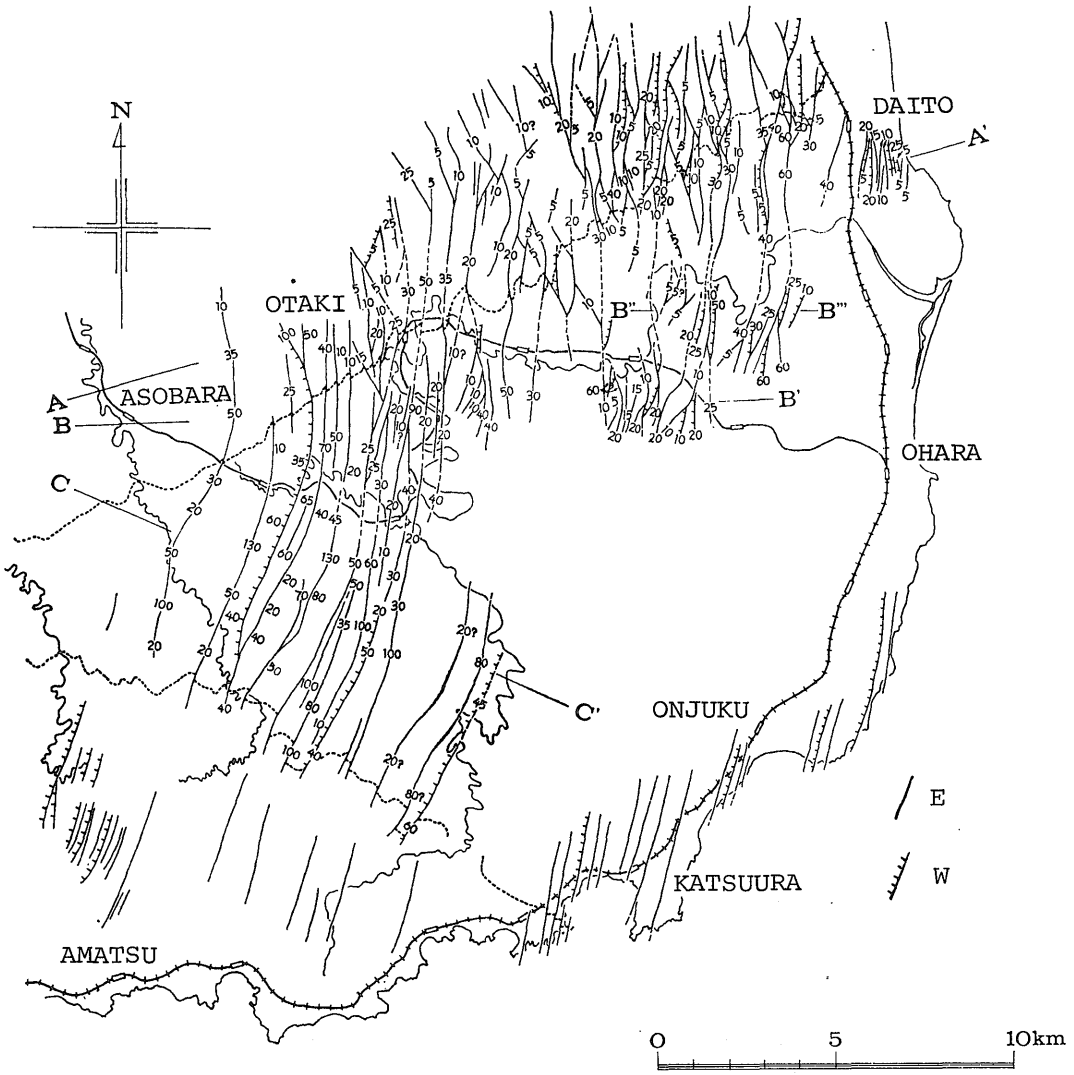

Fig. 2 Distribution of the "major" faults in the eastern part of Boso Peninsula (after MFRG, 1973). Numerals represent the amount of downthrow in meters. W: westside-downthrown fault, E: eastside-downthrown fault.

faults obtained by MFRG (1973) shown in Table 1, graphs on the distribution of the number N of faults with magnitude of throw between T and $T + \Delta T$ (ΔT is 10 cm in this case) are made up as shown in Fig. 4, which is prepared for each of the eastside-down and the westside-down thrown groups of the conjugate fault system and their sum. As a first approximation, relation between log N (T) and log T seems to be expressed as a linear function, and therefore N seems to be expressed by a power-type distribution such as

$$N(T)dT = KT^{-m}dT, \qquad (1)$$

or

$$\log N(T) = k - m \log T, \qquad (2)$$

where K, k ($= \log K$) and m are constants. Using the least squares method k and m are calculated within the range of 10 cm $\leqq T < 300$

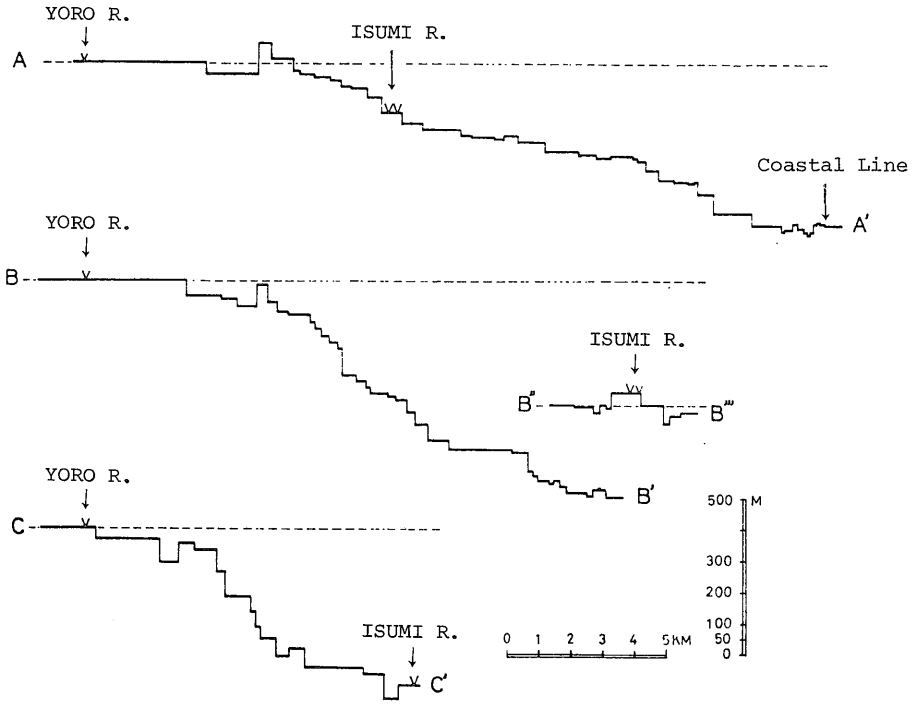

Fig. 3 Schematic profiles showing eastward subsidence due to the "major faults" (after MFRG, 1973). Profile lines are shown in Fig. 2.

cm, and the regression lines are drawn as in Fig. 4.

It is noticeable that the differences among three m-values are fairly significant, whereas k-values are not significantly different between the eastside-down (E-down, for simplicity) and the westside-down (W-down) fault groups. Fig. 5, which is made up from the data on Table 1, is a graphical representation of the cumulative amount of displacement $\sum_{T=0}^{T} N(T) \cdot T$ per 10 cm interval of throw T for the E-down and W-down groups and the sum of, and the difference between them respectively. From this figure and above k- and m-values, it is deduced that in the minor faults the E-down group tends to occur more frequently than the W-down one and that the larger is the fault slip, the more marked the tendency. When we compare Fig. 5 with Fig. 3 this tendency is likely to exist in the major faults as well.

On the process of calculating k- and m-values and drawing the best-fit lines, frequency data of throw smaller than 10 cm (plotted as triangle marks in Fig. 4) are omitted because of statistic insufficiency of sampling as mentioned above. A more strict sampling was carried out by the writer along a road near Onjuku (A′ in Fig. 1), slightly outside of the area studied by MFRG (1973). The road is about 1,000 m long and 515 m of it is composed of road-cut walls where the minor faults are entirely observable. The trend of road is nearly NW–SE and is roughly perpendicular to the strike of the Younger Normal Faults. At these walls, faults of which the downthrow (vertical separation) is larger than one centimeter are wholly collected so that the density of fault development can be calculated. From the data shown in Table 2 k- and m-values are calculated for the sum of the E-down and W-down faults as shown in Fig. 6. In this calculation, frequency data on

faults whose throw is larger than 1 cm are all included. It seems clear that, when we collect samples statistically, the m-value is applicable enough for the faults with throw larger than one centimeter. It is likely that the deviation of frequency N against the throw range of smaller

Table 1 Frequency distribution of minor faults in CASE-A with respect to downthrow. Data in parentheses are not included for calculation of k- and m-values.

Throw (cm)	Eastside-down Group	Westside-down Group	Total
$T<10$	(131)	(124)	(255)
$10\leq T<20$	70	59	129
$20\leq T<30$	34	30	64
$30\leq T<40$	23	26	49
$40\leq T<50$	17	8	25
$50\leq T<60$	11	10	21
$60\leq T<70$	14	2	16
$70\leq T<80$	10	6	16
$80\leq T<90$	7	2	9
$90\leq T<100$	2	1	3
$100\leq T<150$	25	11	36
$150\leq T<200$	6	3	9
$200\leq T<250$	14	6	20
$250\leq T<300$	3	2	5
$300\leq T<350$	7	0	7
Total	374	290	664
$350\leq T$	(4)	(1)	(5)
Ground Total	378	291	669

Table 2 Frequency distribution of downthrow for the minor faults of Younger Normal Fault System observed at a road-cut wall, near Onjuku.

Throw (cm)	E-side-down Group	W-side-down Group	Total
$1\leq T<10$	54	43	97
$10\leq T<20$	11	12	23
$20\leq T<30$	10	10	20
$30\leq T<40$	0	2	2
$40\leq T<50$	1	2	3
$50\leq T<60$	1	1	2
$60\leq T<70$	1	1	2
$70\leq T<80$	0	0	0
$80\leq T<90$	0	0	0
$90\leq T<100$	2	0	2
$100\leq T<150$	1	2	3
$150\leq T<200$	1	0	1
$200\leq T<250$	1	2	3
$250\leq T<300$	1	1	2
$300\leq T<350$	0	1	1
Total	84	77	161
$350\leq T$	(2)	(0)	(2)
Ground Total	86	77	163

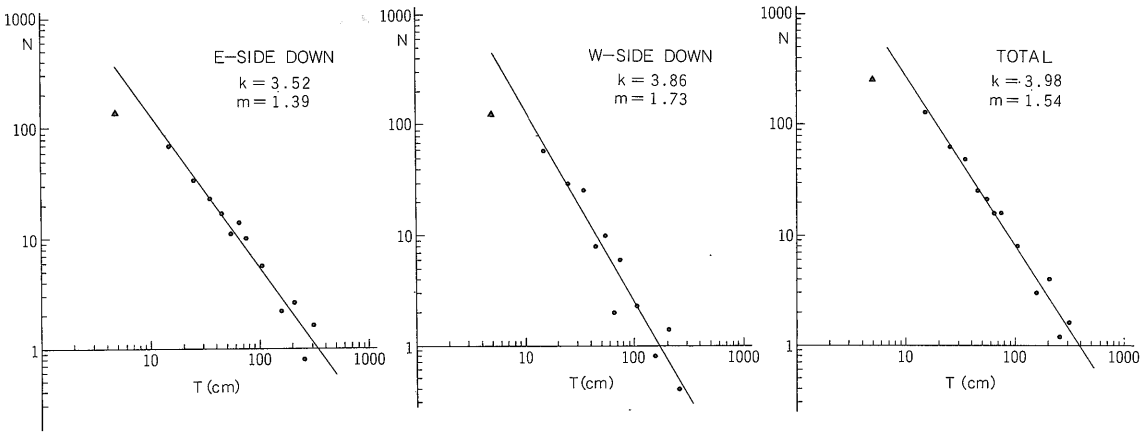

Fig. 4 Relations between the throw T and its number $N(T)$ for the minor faults in CASE-A. Solid triangle mark represents the number of faults having throw smaller than 10 cm, which is excluded for calculating k- and m-values.

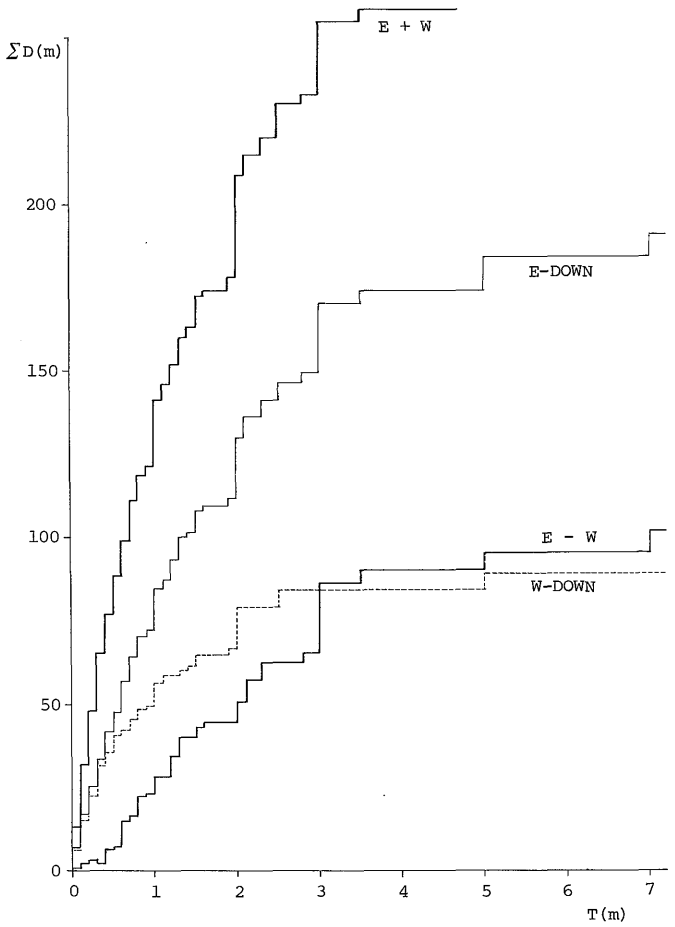

Fig. 5 Cumulative curves of displacement against throw for the minor faults in CASE-A.

than 10 cm from the regression lines in Fig. 4 is not due to a real change in characteristics of these smaller faults but merely due to insufficiency of sampling. As for the faults with throw smaller than one centimeter, however, the frequency N does not increase but tends to decrease as far as the writer observed at this site.

2) CASE-B: Younger Normal Faults in the northern part of Miura Peninsula

In this area including Zushi and Yokosuka Cities and Hayama Town, the stress field and other tectonic conditions related to faults of this system had been investigated by KAKIMI *et al.* (1966). The shear angles obtained from the conjugate faults are very small, 32° on an average value. This and other modes of occurrence imply that the Younger Normal Faults in this area were generated under more brittle state than those in CASE-A. Among three axes of principal stresses obtained, the direction of the maximum tension axis is comparatively stable and indicates around WNW–ESE direction which is parallel to the general structural trend of Miura Peninsula. Besides, it gently plunges toward east and west in harmony with undulation of the longitudinal structural trend (KAKIMI *et al.*, 1966). Directions of other two principal axes are, however, rather unstable and tend to rotate about the axis of maximum tension. From these stress distributions the

writer (KAKIMI, 1975) pointed out that the Younger Normal Faults in this area had occurred as a special type of the conical faults under some unstable stress conditions. Therefore, the net-slip of these faults is purely of normal-slip in some places, but in other places it has large component of strike-slip.

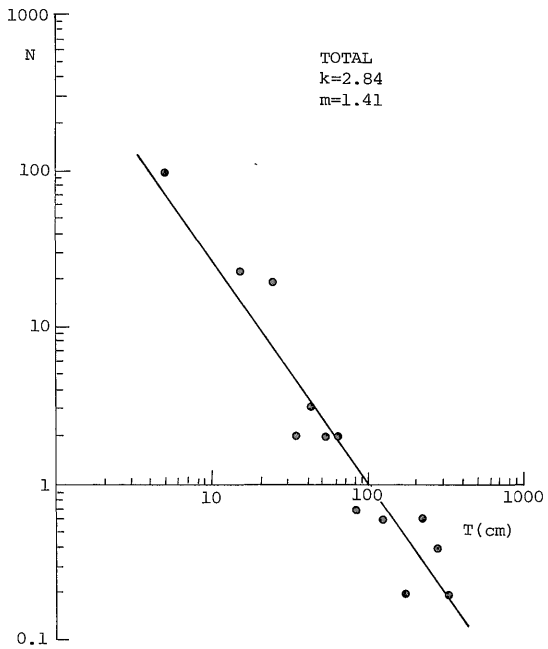

Fig. 6 Relation between the throw T and its number $N(T)$ for the Younger Normal Faults observed at road-cut walls near Onjuku.

Table 3 shows the frequency of faults at every interval of 10 cm in throw. Fig. 7 and Fig. 8 are prepared from the data on Table 3 under

Table 3 Frequency distribution of minor faults in CASE-B with respect to downthrow. Data in parentheses are not used for calculation of k- and m-values.

Throw (cm)	E-side-down Group	W-side-down Group	Total
$T < 10$	(218)	(237)	(455)
$10 \leq T < 20$	125	180	305
$20 \leq T < 30$	41	68	109
$30 \leq T < 40$	30	32	62
$40 \leq T < 50$	25	41	66
$50 \leq T < 60$	20	20	40
$60 \leq T < 70$	13	8	21
$70 \leq T < 80$	8	8	16
$80 \leq T < 90$	4	2	6
$90 \leq T < 100$	2	4	6
$100 \leq T < 150$	12	29	41
$150 \leq T < 200$	5	7	12
$200 \leq T < 250$	4	4	8
$250 \leq T < 300$	0	1	1
$300 \leq T < 350$	1	2	3
$350 \leq T < 400$	0	2	2
Total	508	645	1,153
$400 \leq T$	(12)	(7)	(19)
Ground Total	520	652	1,172

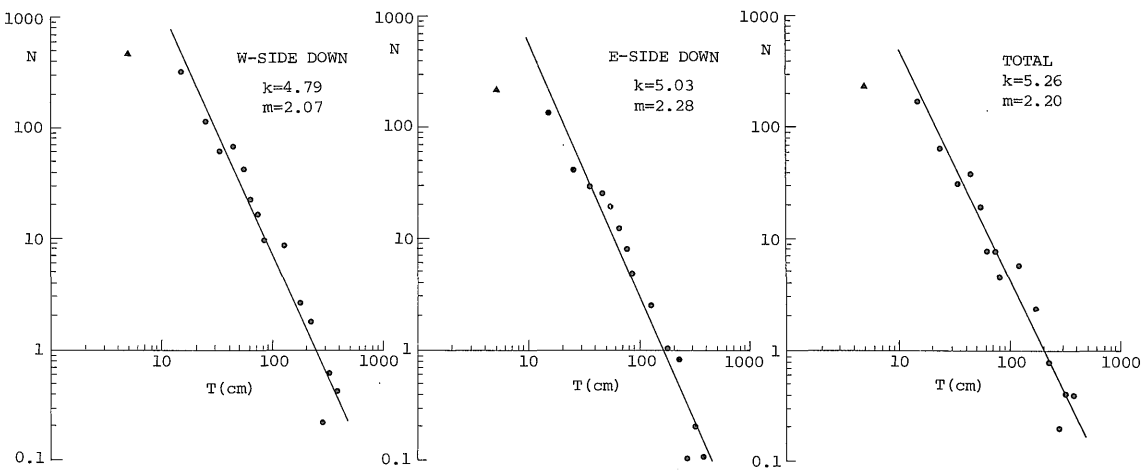

Fig. 7 Relations between the throw T and its number $N(T)$ for the minor faults in CASE-B.

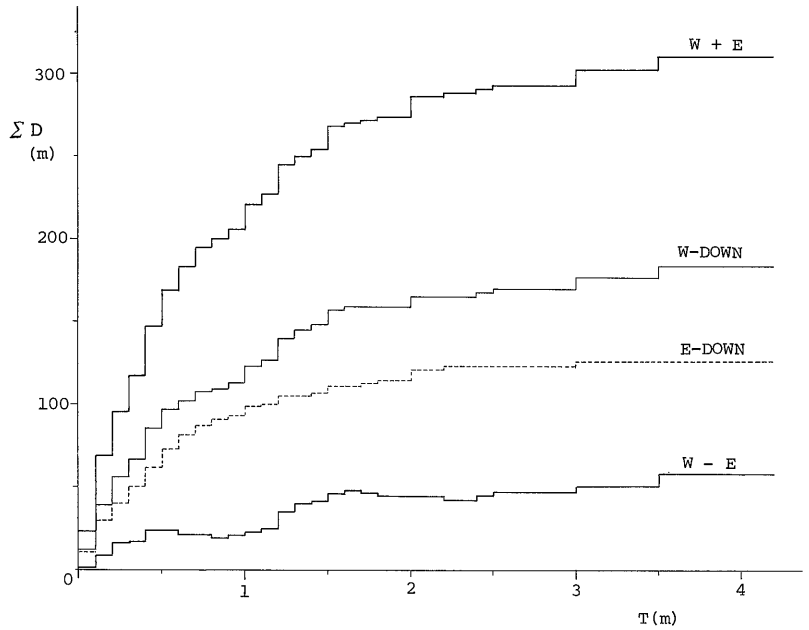

Fig. 8 Cumulative curves of displacement against throw for the minor faults in CASE-B.

the same processes as in CASE-A, and calculated *k*- and *m*- values are shown in Fig. 7. As clearly shown in Table 3 and Fig. 8, both fault frequency and accumulated amounts of throw for the W-down faults are larger than those for the E-down faults. The *m*-value of the E-down faults in this case is significantly larger than that of the W-down faults, contrary to the CASE-A. These may suggest the opposite mode of deformation by faulting between Boso and Miura Peninsulas.

3) CASE-C: Younger Normal Faults at the southern tip of Miura Peninsula

At the uplifted abrasion platform around Jogashima Island located at the southern tip of Miura Peninsula, minor faults belonging to some of four systems are developed abundantly in the alternation strata of mudstone and volcaniclastic sandstone of the Miura Group. Among them the Younger Normal Faults are the most predominant.

According to KODAMA (1968, 1974) the Younger Normal Faults are of comparatively large downthrow, the largest amount of which is up to 3.5 m at a platform observed, and of thick shear zone composed of many sheets of smaller fault plane. They sometimes are branched-off and separated to several faults of smaller slip and are re-connected to a single fault of larger slip and thick shear zone. These suggest that faulting had progressed repeatedly even in minor faults. In this district, the W-down group is more predominant in number as well as in amount of throw than the E-down one. The shear angle is about 40° in an average value which is similar to that in the CASE-A.

Relation between frequency and magnitude of throw of the Younger Normal Faults is shown in Fig. 9 which was prepared by KODAMA (1974) for those developed in Jogashima Island and Misaki district. *k*- and *m*-values are shown in Fig. 9. The *m*-value for the W-down faults seems to be significantly smaller than that for the E-down faults. This result is compatible with that the W-down faults are more predominant than those of the opposite sense, as mentioned above. Fig. 10 is another expression of the predominancy of the W-down faults over the E-down faults, and the mode of deforma-

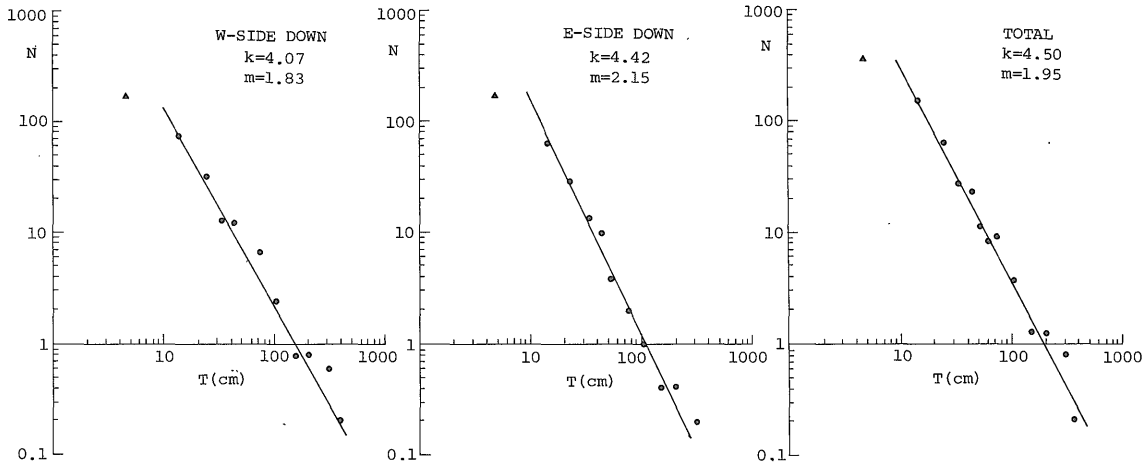

Fig. 9 Relations between the throw T and its number $N(T)$ for the minor faults in CASE-C (redrawn from KODAMA, 1975).

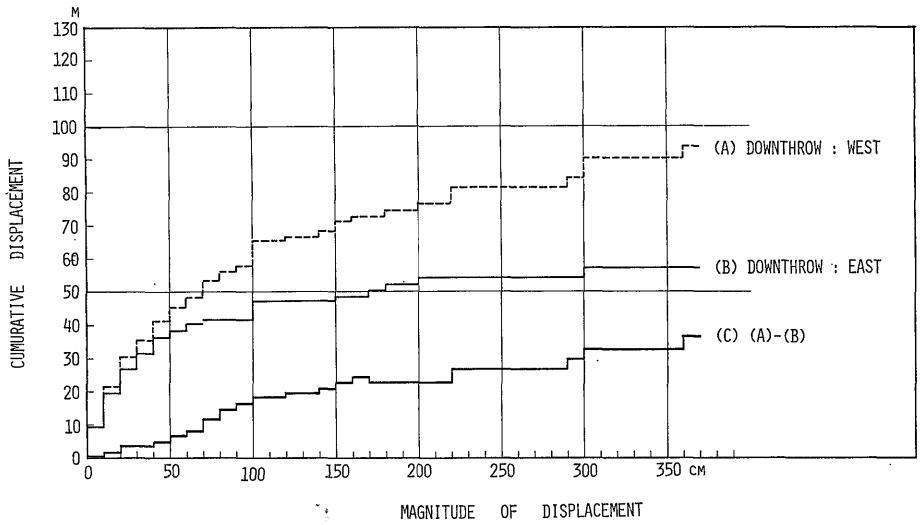

Fig. 10 Cumulative curves of displacement against throw for the minor faults in CASE-C (after KODAMA, 1975).

tion in this area.

4) CASE-D: Older Reverse Faults in the northern part of Miura Peninsula

The area in which the Older Reverse Faults are frequent and the area where the Younger Normal Faults treated in CASE-B occur, just overlap to each other. This area is situated tectonically on the northern limb of the Hayama Uplift Zone. The stress field and other tectonic conditions related to these faults were studied by KAKIMI *et al.* (1966). Most of these faults have general strike of E–W to NW–SE and are divided into the northside-up and southside-up groups forming a conjugate fault system, but partly, especially at the northernmost part, they have variable strikes and make up a conical fault system of R–W type (KAKIMI, 1974). Thus, considering the existence of conical faults in part, the axis of maximum compression

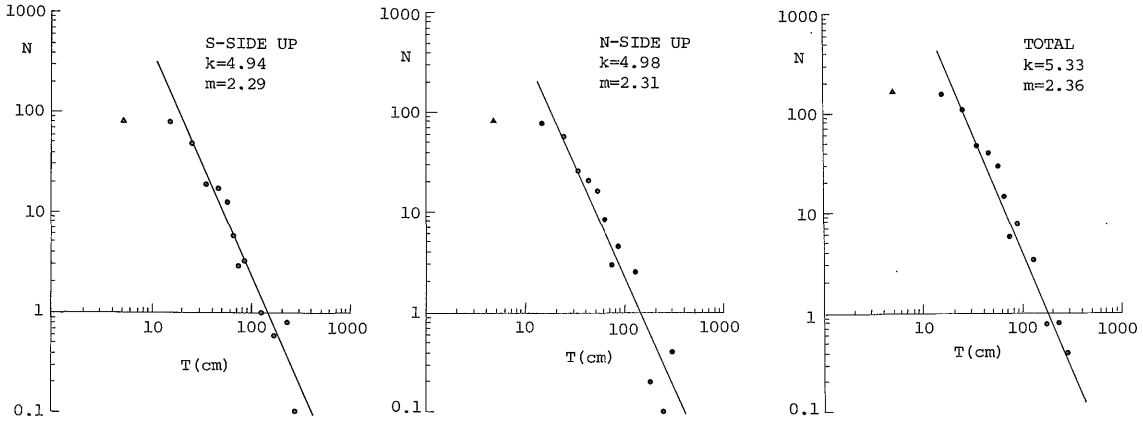

Fig. 11 Relations between the throw T and its number $N(T)$ for the minor faults in CASE-D.

Table 4 Frequency distribution of minor faults in CASE-D with respect to upthrow. Data in parentheses are not included for calculation of k– and m–values.

Throw (cm)	Southside-up Group	Northside-up Group	Total
$T < 10$	(85)	(87)	(172)
$10 \leq T < 20$	81	83	164
$20 \leq T < 30$	51	59	110
$30 \leq T < 40$	20	27	47
$40 \leq T < 50$	18	22	40
$50 \leq T < 60$	13	17	30
$60 \leq T < 70$	6	9	15
$70 \leq T < 80$	3	3	6
$80 \leq T < 90$	3	9	12
$90 \leq T < 100$	4	2	6
$100 \leq T < 150$	5	13	18
$150 \leq T < 200$	3	1	4
$200 \leq T < 250$	4	0	4
$250 \leq T < 300$	0	2	2
$300 \leq T < 350$	0	0	0
$350 \leq T < 400$	0	1	1
Total	296	335	631
$400 \leq T$	(2)	(4)	(6)
Ground Total	298	339	637

indicating nearly N–S is relatively stable but the other principal stress axes are rather unstable.

Table 4 and Fig. 11 show the frequency distribution of upthrow[2] in the Older Reverse Faults. On the occasion of calculating m- and k-values, frequency of faults whose throw is samller than 10 cm is not included because the data which are plotted on Fig. 11 by solid triangle marks deviate distinctly from the best-fit lines. However, since in this case the number of faults whose throw is in the range $10 \leq T < 20$ cm seems to be also less sufficient, such large deviation in smaller faults may not be merely due to insufficiency of sampling as examined in CASE-A, but may be attributed to an essential characteristics of the faulting in this system.

As shown in Table 4, the northside-upthrown (N-up) group is slightly larger in number than the southside-up (S-up) one. This tendency is represented also in Fig. 12 which shows cumulative displacement $\sum_{T=0}^{T} N(T) \cdot T$ per 10 cm interval of throw T for the N- and S-up groups. These are incompatible apparently with that this area is situated on the northern limb of the Hayama Uplift zone where it is expected that the southside-up movement is predominant. However, since the collected data are not strictly statistic, it is not affirmed whether these differences in number and cumulative displacement are really significant or not. In so far as

[2] Vertical component of reverse separation is conventionally called upthrow in this case.

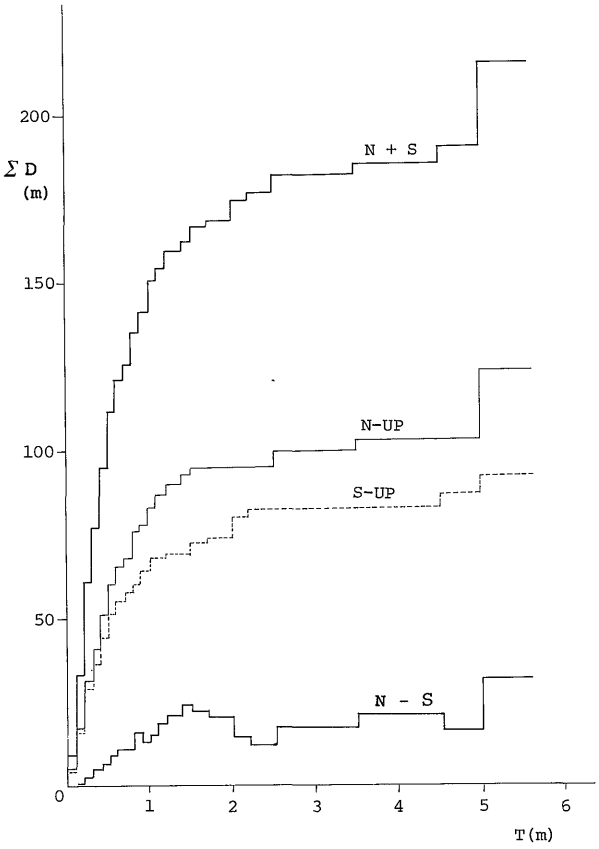

Fig. 12 Cumulative curves of displacement against throw for the minor faults in CASE-D.

m-values shown in Fig. 11 are concerned, there are no significant difference between N-up and S-up groups of these faults.

4. Discussions

1) An approach to the quantitative estimation of crustal deformation by fault slip

Equation (1) or (2) can be regarded as a consequence of representing the spectrum of the crustal deformation borne by faulting. If the empirical Eq. (1) holds good throughout a throw-range in question, we could estimate the distribution of crustal deformation of the given area more or less quantitatively. The total displacement D of which the magnitude of throw (displacement in each fault) is between T and $T + dT$ can be written from Eq. (1) as

$$D(T)dT = N(T)TdT = KT^{-m+1}dT. \quad (6)$$

In this equation, if m is larger than 1, total displacement D becomes smaller with the increase in throw T. When m is equal to 1, D will be a constant value regardless of the amount of T. And, if m is smaller than 1, D becomes larger with the increase in T. Since m-values are always larger than 1 for the cases treated in this paper, the mode of crustal deformation may be such that the total amounts of displacement by larger faults are rather smaller than those by smaller faults so far as we use the equal intervals for throw scale. It is interesting that this result is quite similar to the relation of total seismic energy annually released to each energy level which was pointed out by ASADA *et al.* (1951) as

$$N(E)EdE = \text{const.} \times E^{-0.5}dE, \quad (7)$$

where $N(E)E$ is the total energy annually released in shallow earthquakes having the energy between E and $E + dE$. Thus we can say from Eq. (7) that the annual total energy becomes smaller with the increase in E, if the earthquakes are classified at equal intervals of energy scale.

From Eq. (6) it is deduced that the accumulated amount of displacement $\sum_{T=T_1}^{T_2} D(T)dT$ of which the range of throw is between T_1 and T_2 is expressed as

$$\sum_{T=T_1}^{T_2} D(T)dT = \sum_{T=T_1}^{T_2} N(T)TdT,$$

or

$$\int_{T_1}^{T_2} D(T)dT = \int_{T_1}^{T_2} KT^{-m+1}dT = C \times [T^{-m+2}]_{T_1}^{T_2}, \ (T \neq 0), \quad (8)$$

where C is the numerical constant and equal to $K/(-m+2)$.

Fig. 13 represents the curves of cumulative displacement $\sum_{T=T_1}^{T_2} D$ against T_2 for variable m-values when both C and T_1 are equal to unity. As shown in Fig. 13, if m is larger than 1, the curves are convex upwards. Therefore, the rate of increase in cumulative displacement $\sum D$ becomes smaller with the increase in T. Since

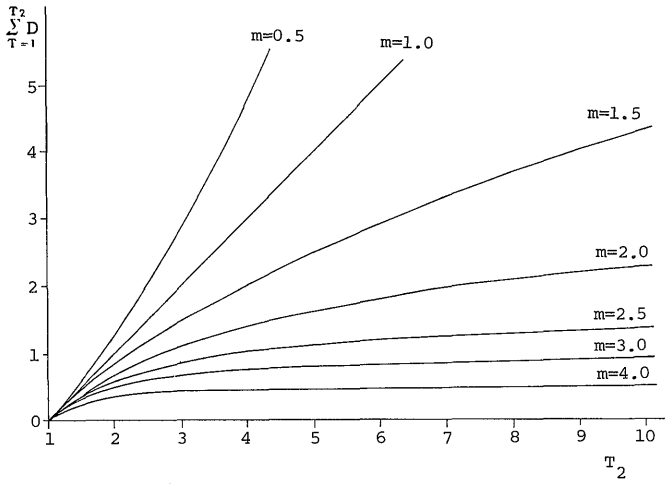

Fig. 13 Curves of cumulative displacement $\sum_{T=1}^{T_2} D$ against throw T_2 for variable m-values when C and T_1 in Eq. 8 are put as unity.

m is larger than 1 in all cases treated in the previous chapter, the curves of cumulative displacement actually measured are convex upwards as shown in Figs. 5, 8, 10 and 12. Thus, if Eq. (1) holds for all the ranges from the smallest to the largest throws, we could estimate the whole displacement in a certain area surveyed, so far as m- and k-values can be obtained with accuracy. In practice, however, it would be difficult to obtain k-value of Eq. (1), because k is a value concerned with the density of fault development which is apt to vary from place to place.

In the eastern part of Boso Peninsula described in CASE-A, the amount of displacement of the major faults, the throw of which is larger than 10 meters, is well known by detailed geological surveys (Mitsunashi *et al.*, 1961; Ishiwada *et al.*, 1971). The accumulated amount of vertical displacements $\sum D$ at A–A′ line in Fig. 2 is about 650 m for the E-down fault group and about 150 m for the W-down one respectively, and the difference between both groups, namely, the amount of eastward subsidence, is about 500 m as shown in Fig. 3. Assuming that m-values, m_E (= 1.39) and m_W (= 1.73) for the E-down and W-down fault groups obtained from the minor faults, hold as well for the major faults of which the throw-range is between 10 m and 100 m[3], we can estimate C-values from the following equations as

$$\sum_{T=10\mathrm{m}}^{100\mathrm{m}} D(T)dT = C_E[100^{-m_E+2} - 10^{-m_E+2}] = 650 \text{ (m)}$$

and

$$\sum_{T=10\mathrm{m}}^{100\mathrm{m}} D(T)dT = C_W[100^{-m_W+2} - 10^{-m_W+2}] = 150 \text{ (m)},$$

where C_E and C_W are C-values in Eq. (8) for E-down and W-down faults respectively. Consequently, the total amount of displacement both by minor and major faults can be obtained using these C-values. In the case of A–A′ line in Fig. 3, the differential amount of regional displacement obtained by subtracting the amount of cumulative displacement of W-down group from that of E-down group is about 500 m in the sense of eastward subsidence. The total amount of horizontal stretch due to normal faulting among A–A′ line, about 20 km in length, will be about 400 m which is obtained from the operation of following equation

[3] As shown in Figs. 2 and 3, the maximum amount of downthrow is approximately 100 meters in both E-down and W-down fault groups treated here.

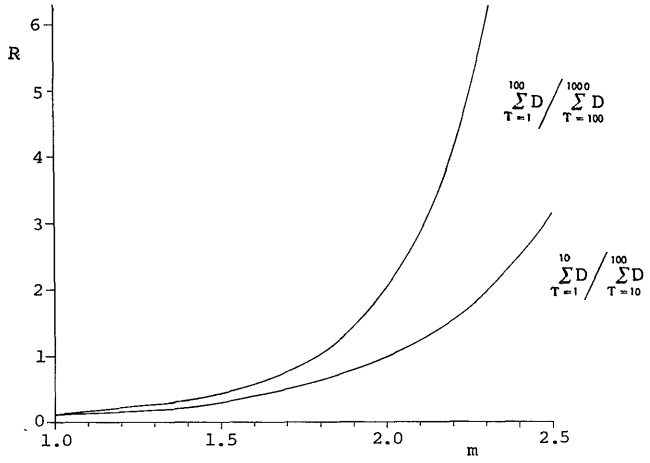

Fig. 14 Curves of ratio R of the cumulative displacement for the smaller faults to that for the larger faults against m-value.

$$\cot\theta\left[\sum_{T=10\mathrm{m}}^{100\mathrm{m}} D(T_{\mathrm{E}})dT+\sum_{T=10\mathrm{m}}^{100\mathrm{m}} D(T_{\mathrm{W}})dT\right], \tag{9}$$

where T_{E} and T_{W} mean throws of E-down and W-down fault groups respectively, and θ is the mean angle of fault dip which is 70° in this case.

If m-value is assumed as the same value on the whole throw range, we can calculate the ratio of cumulative displacement for the smaller faults to that for the larger faults from the Eq. (8). In the case mentioned above, the ratio R of the cumulative displacement for the smaller faults of the throw range of 10 cm $\leq T <$ 10 m to that for the larger faults having throws of 10 m $\leq T <$ 100 m is 0.31 for the E-down faults, and 0.83 for the W-down faults. These ratios can be obtained solely from m-values regardless of C- or k-values as shown in Fig. 14. If m is larger than 1.8 the ratio R becomes larger than 1, and when m is 2.5, R becomes much larger than 10. Thus, minor faults should never be negligible for the purpose of estimating the regional deformation quantitatively.

2) Significance of m-value as an indicator of fracturing conditions

It is asserted by many investigators such as Miyamura (1962) that the regional variations in b-values in Gutenberg-Richter's formula (Eq. 1) or m-values in Ishimoto-Iida's formula (Eq. 2) are related to geotectonic structures, although the skeptic opinions that these variations are mainly attributed to the statistical insufficiency, are supported by some investigators (e.g., see Utsu, 1971). For example, it has been well known that the m-value is exceptionally large in the volcanic earthquakes of very shallow foci.

Mogi (1962) discussed the physical meanings of m- or b-value on the basis of laboratory experiment on brittle fracturing of various materials. According to his experiments, the magnitude-frequency relation of elastic shocks accompanying the fracturing satisfies the Ishimoto-Iida's formula in many cases. The m-values vary in the wide range from 0.3 to 2.7 dependent mainly upon the mechanical structures of medium and the applied stress states. The log n - log a relation, in which n is the number and a is the maximum trace amplitude of shock, is linear for the heterogeneous solids having irregular structures, and m-value increases with the increase in degree of heterogeneity which is equivalent to the increase in local concentration of applied stress. On the other hand, the log n - log a curve is often concave downwards for solids having some

Table 5 *m*-values and tectonic conditions for the minor faults developed in different regions

Case	Region	Sense of fault-slip	*m*-values			Average angle of shear	Ductility	Stability in stress state
			For one of the conjugate pair		For total			
A	E. Boso Pen.	Normal	(E-down) 1.39	(W-down) 1.73	1.54	40°	Brittle	Stable
B	N. Miura Pen.	Normal*	(W-down) 2.07	(E-down) 2.28	2.20	32°	Verry brittle	Unstable
C	S. Miura Pen.	Normal	(W-down) 1.83	(E-down) 2.15	1.95	40°	Brittle	Stable
D	N. Miura Pen.	Reverse*	(S-up) 2.29	(N-up) 2.31	2.36	83°	Ductile	Unstable

* Including the strike-slip component.

regular structures. Particularly in a block structure, the curve is composed of two straight lines intersecting at the amplitude which is related to the unit dimension of the block structure (Mogi, 1962, 1967).

In this section, the present writer would like to examine the relation between the variations in *m*-values and the tectonic conditions under which minor faults had generated. The *m*-values and other characteristics suggesting the fracturing conditions for each fault-system treated in the previous chapter are shown in Table 5. Although any definite conclusion is not deduced yet because of the statistical insufficiency, the following tendencies may be recognized.

When we compare the *m*-values for the whole faults, *m* seems to be independent of ductility of materials as shown in Table 5 in which a wide range of ductility from very brittle to very ductile states is treated. On the other hand, *m*-value seems to be related to the spatial variation in stress distribution, namely, *m* is small when applied stress is rather stable so that the parallelism of fault plane is fairly good as shown in CASE-A and -C, and *m* is large in the other cases in which the stress state is unstable so that the local variation in strike and dip of fault is markedly large. This tendency is conformable to one of Mogi's (1962) results.

Another problem is that the log N - log T relation is not expressed by a straight line but is expressed by a curve convex upwards or two straight lines. This tendency is likely to be recognized in such cases as the W-down group of CASE-A, E-down group of CASE-B, and both N-up and S-up groups of CASE-D. In every case, the amount of throw T corresponding to the intersecting point of two straight lines is around several tens of centimeters. According to Mogi (1962), this tendency may correspond to such cases that the faults occurred in the medium having some regular structures. If so, what is the "ragular" structure in the present cases? Considering that the Miura and Kazusa Groups are composed mainly of the alternation of sandstone and siltstone in which the sandstone is almost unconsolidated, whereas the siltstone is moderately consolidated, the "regular" structure may indicate the layered structure different in the degree of consolidation between sandstone and siltstone.

However, it should be careful that the n - a relations in seismicity and Mogi's experiments for elastic shocks fundamentally differ from the N - T relation for the throw of fault in such point that the throw itself is probably the result of multiple slips even in the minor faults. Around this point the writer will discuss in the next section.

From another standpoint, Nagumo (1969a, b) pointed out that the Ishimoto-Iida's formula (Eq. 3) is theoretically derived from a deformation-fracture relation. His basic assumptions are that the number of earthquakes is proportional to the curvature of the plastic deformation of the medium, and the size of earthquake is governed by the structural wavelength, namely, the larger earthquake is produced by the structure of the longer wavelength.

Thus, the power function representation of Ishimoto-Iida's formula is due to the same representation for the spectrum of plastic deformation of the medium. The coefficient m indicates the sharpness of the spectrum of deformation, that is, m-value in Eq. (3) is large when the crustal deformation is sharp and small in scale, whereas it is small when the deformation includes the components of long wavelength.

As shown in Table 5, m–values in Eq. (2) for the Younger Normal Faults in Miura Peninsula (CASE-B and -C) are significantly larger than those in Boso Peninsula (CASE-A). On the other hand, it has been found in the previous studies that the deformation pattern along the direction perpendicular to the strike of the Younger Normal Faults in CASE-A is gentle but large in scale as shown in Fig. 3, whereas the pattern in CASE-B shows the undulation with relatively short wavelength which is represented typically on a structural profile made by KAKIMI *et al.* (1966). Besides, KODAMA (1974) clarified using the topographic profiles for both peninsulas and surrounding sea bottoms that the area of CASE-A is situated at the eastern shoulder of a large slope dipping gently towards the eastern continental slope, whereas the area of CASE-C is located at the western shoulder of a steep slope having small radius of curvature.

Thus, according to NAGUMO's arguments, the difference in m-values for the Younger Normal Faults between Miura and Boso Peninsulas is likely due to the difference in sharpness of deformation between both peninsulas.

3) Change in m-value corresponding to the progressive increase in fault displacement

Since the throw in each fault is considered to be a result of repeated slips even in the minor faults as shown in CASE-C, m-value (and k-value, as well) may vary during the periods of fault development. Remembering the concept of "maturity" of fault development (KAKIMI and KINUGASA, 1977) and many results of laboratory experiment on fracturing, minor faults distributing uniformly over a wide area can be considered as the products at the initial "immature" stage of crustal deformation. In the next stage, fracturing will concentrate to a relatively large faults in a few narrow zones and the "major" faults will take place (TSUNEISHI *et al.*, 1975). It has been found in the studies on earthquake faults that there is an upper limit of single slip of faulting for a given fault system as well as a lower limit of it, when aseismic fault-creep is disregarded. For example, MATSUDA (1975) proposed that the amount of unit displacement d accompanying an earthquake has a relation with the earthquake magnitude M roughly as

$$\log d \text{ (meter)} = 0.6M - 4.0$$

for Japanese inland earthquakes. According to his empirical formula, if the upper limit of earthquake magnitude is equal to 7 for a region concerned, the upper limit of unit displacement amounts about 1.6 meters. In the case of the Younger Normal Faults in Boso and Miura Peninsulas, the upper limit of single fault-slip is likely to be smaller than one meter, since the faults were developed under a tensional stress field at very shallow depth so that the magnitude of energy release from the single slip is also small in this case. If we assume that the distribution of unit displacement follows the Eq. (2) on the range below the upper limit d_{max} of faults, $\log N$ - $\log T$ relation is expressed as a straight line with large m-value truncated at d_{max}. As MOGI (1962) pointed out, the magnitude of d_{max} may be related to some "regular" mechanical structures such as layered structure composed of the alternation strata with different degrees of consolidation. Corresponding to the progressive faulting, the faults with throw larger than d_{max} will take place and increase gradually in number and $\log N$ - $\log T$ relation will be represented with a curve convex upwards or two straight lines for different throw ranges, as shown schematically in Fig. 15. The amount of throw T^* corresponding to the intersection point of the two lines will be equal

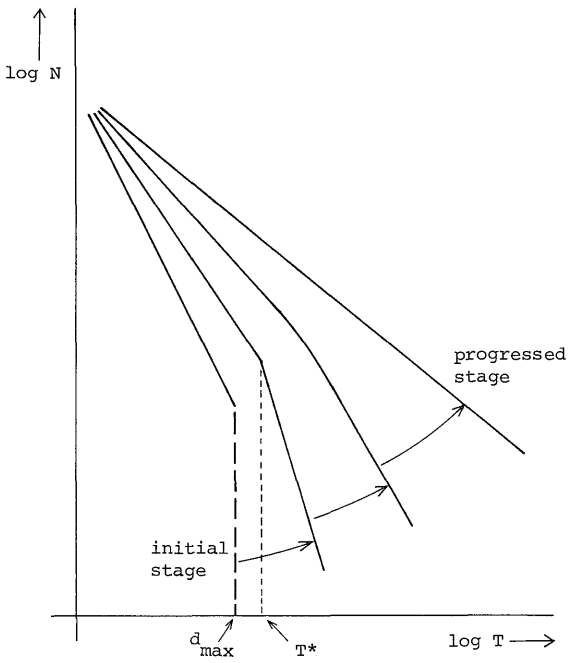

Fig. 15 Changes in the log N -log T curves corresponding to the progressive development of faulting.

to, or somewhat larger than the maximum unit displacement d_{max} of a fault system.

In the more "matured" stage of faulting, it is expected that the slip movement will take place along the faults with larger throw and the faults with smaller throw will cease further development. Consequently, the log N - log T curve will gradually become close to a straight line, and m-values will be decreased with the increase in the "maturity" of faulting.

As for the minor faults in Boso Peninsula (CASE-A), the log N - log T curve is likely to be upward convex for the W-down group in the conjugate fault system and the amount of T^* corresponding to the inflexion point of assumed two lines is approximately several tens of centimeter. If so, it is likely that the upper limit d_{max} of the unit displacements in this system amounts also to around several tens of centimeter. On the contrary, log N - log T relation in the E-down group is expressed as a single straight line rather than a curve convex upwards.

Thus, we may distinguish the development stages in faulting by means of examining the m-values and the form of log N - log T curve. Although two fault sets of a conjugate fault system are equivalent to each other for the stress field which initiates minor faults, they are not always equivalent to each other for the "deformation field" under which displacement develops. In the early immature stage of faulting, the m-value will be large and the log N - log T relation will be represented with two straight lines for both sets of a conjugate system. In the more matured stage, either one of the two sets becomes to develop predominantly in harmony with the regional deformation so that the m-value decreases and the log N - log T curve becomes close to a straight line, whereas the other set remains relatively at the earlier stage.

5. Summary and Conclusion

Magnitude-frequency relation for the displacement of minor faults is examined in several cases among which the faulting conditions, such as stress state, sense of fault-slip, ductility of materials etc., are different from each other. In each case the number N of the faults with throw between T and $T + dT$ is expressed approximately for a certain throw range by a power-type equation as

$$N(T)dT = KT^{-m}dT, \qquad (1)$$

or

$$\log N(T) = k - m \log T, \qquad (2)$$

where K, k and m are the numerical constants. In the cases treated in the present paper, calculated m-values fall into a wide range of 1.3 to 2.4.

If these equations hold good for a certain area and throw range in question, we could estimate the distribution of crustal deformation of the area more or less quantitatively. The coefficients K and k are the function of area and the density of fault displacement which is related to the intensity of regional deformation. The exponent m indicates the spectral structure

on the magnitude of fault displacement which is actually related to the tectonic conditions in the faulted region, such as the homogeneity of mechanical structure, stability of stress distribution, sharpness of regional deformation, etc. So far as the writer examined in the cases treated above, the difference in m-value is likely to reflect well the tectonic conditions, and the results are coincident, to a certain degree, with those deduced by MOGI (1962) and NAGUMO (1969) with respect to the magnitude of elastic shocks (earthquakes).

If m-value is larger than 1, the portion of crustal deformation by the larger faults is rather smaller than the portion by the smaller faults so far as we adopt the equal intervals for throw scale. When m is larger than 2.0, the total displacement by the smaller faults becomes always larger, even if we adopt the logarithmic intervals for throw scale. Thus, minor faults should never be negligible for the quantitative estimation of regional deformation.

Since the displacement in each fault is a result of repeated slips and the faulting itself is considered to change its mode with time, N-T relation in Eq. (1) may vary with time corresponding to the degree of progressive deformation. In the earlier (immature) stage of faulting, the m-value will be large and the log N - log T relation will be represented by a truncated line or two straight lines for both sets of a conjugate fault system. In the more matured stage, either one of the conjugate sets which is compatible with the regional deformation, will become predominant so that the m-value decreases and the log N - log T curve becomes close to a straight line through a curve convex upwards, whereas the other set still remains at the earlier stage.

In conclusion, it can be stated that the magnitude-frequency relation for fault displacement expressed by the Eq. (1) or (2) is not only useful for the estimation of regional tectonic conditions but for the estimation of temporal changes in them, as well as the Gutenberg-Richter's formula is so for the examination of regional and temporal variations in seismicity.

Acknowledgement

This study is a part of the writer's doctorial thesis presented at the Faculty of Science, Hokkaido University. The writer wishes to express his hearty thanks to professor MASAO MINATO of Hokkaido University for his continuous encouragement throughout this study. He also express his sincere thanks to Dr. K. KODAMA and Dr. H. KOIDE of the Geological Survey of Japan for their kind advice and discussion for the significance of magnitude-frequency relations on faulting and seismicity. Thanks are also due to Mr. Y. KINUGASA and other members of the Seismotectonics Research Section of the Geological Survey who are assisting with all aspects of the writer's study. Most of the figures were drafted by Mr. Y. MIYAZAWA.

References

ASADA, T., SUZUKI, Z. and TOMODA, Y. (1951) Notes on the energy and frequency of earthquakes. *Bull. Earthq. Res. Inst.*, vol. 29, p. 289–293.

GUTENBERG, B. and RICHTER, C. F. (1944) Frequency of earthquakes in California. *Bull. Seism. Soc. Am.*, vol. 34, p. 185–188.

ISHIMOTO, M. and IIDA, K. (1939) Observations sur la séismes enregistrés par le microsismographe construit dernièrement (1). *Bull. Earthq. Res. Inst.*, vol. 17, p. 443–478.

ISHIWADA, Y., MITSUNASHI, T., SHINADA, Y. and MAKINO, T. (1971) Mobara. Geological maps of oil and gas field of Japan, 10, Geological Survey of Japan.

KAKIMI, T. (1974) Temporal changes in Quaternary stress field in the South Kanto district, in KAKIMI, T. and SUZUKI, Y., eds., *Seismicity and crustal movement in Kanto Province*, Lattice Co. Ltd., Tokyo, p. 59–70.

——— (1975) The conical faults; their types and examples. *Jour. Geol. Soc. Japan*, vol. 81, p. 39–51.

———, HIRAYAMA, J. and KAGEYAMA, K. (1966) Tectonic stress-fields deduced from the

minor fault systems in the northern part of the Miura Peninsula. *Jour. Geol. Soc. Japan*, vol. 72, p. 469–489.

KAKIMI, T. and KODAMA, K. (1974) Frequency distribution of faults in respect to throw, with special reference to crustal deformations and seismicities (preliminary note). *Bull. Geol. Surv. Japan*, vol. 25, p. 75–87.

——— and KINUGASA, Y. (1976) A geologic significance of the Irozaki earthquake fault, viewed from "maturity" of faulting. *Jour. Geod. Soc. Japan*, vol. 22, p. 278–279.

KINUGASA, Y., KAKIMI, T. and HIRAYAMA, J. (1969) The minor-fault systems on the coastal area of the eastern Boso Peninsula. *Bull. Geol. Surv. Japan*, vol. 20, p. 13–38.

KODAMA, K. (1968) An analytical study on the minor faults in the Jogashima Island. *Jour. Geol. Soc. Japan*, vol. 74, p. 265–278.

——— (1974) Fault development and crustal deformation, in KAKIMI, T. and SUZUKI, Y. eds., *Seismicity and crustal movement in Kanto Province*, Lattice Co. Ltd., Tokyo, p. 71–86.

——— (1975) Fault systems in the southern part of the Miura Peninsula, south of Tokyo. unpublished Ph. D. thesis, Tokyo University of Education.

KOIKE, K. (1955) Geo-historical significance of interformational disturbances. *Jour. Geol. Soc. Japan*, vol. 55, p. 566–582.

MATSUDA, T. (1975) Magnitude and recurrence interval of earthquakes from a fault. *Jour. Seism. Soc. Japan (Zisin)*, ser. II, vol. 28, p. 269–283.

THE MINOR FAULTS RESEARCH GROUP (MFRG) (1973) A minor fault system around the Otaki area, Boso Peninsula, Japan. *Earth Science (Chikyu Kagaku)*, vol. 27, p. 180–187.

MITSUNASHI, T., YAZAKI, K., KAGEYAMA, K., SHIMADA, T., ONO, A., YASUKUNI, N., MAKINO, T., FUJIWARA, K. and KAMATA, S. (1961) Futtsu—Otaki. Geological maps of the oil and gas field of Japan, 4, Geological Survey of Japan.

——— (1968) General Stratigraphy, in *Geologic structures and sedimentary structures in the Miura and Boso Peninsulas*, Geol. Soc. Japan, Excursion Guidebook.

MIYAMURA, S. (1962) Magnitude-frequency relation of earthquakes and its bearing on geotectonics. *Proc. Japan Acad.*, vol. 38, p. 27–30.

MOGI, K. (1962) Magnitude-frequency relation for elastic shocks accompanying fractures of various materials and some related problems in earthquakes, I and II. *Bull. Earthq. Res. Inst.*, vol. 40, I: p. 125–173, II: p. 831–853.

——— (1967) Regional variations in magnitude-frequency relation of earthquakes. *Bull. Earthq. Res. Inst.*, vol. 45, p. 313–325.

NAGUMO, S. (1969a) A derivation of Ishimoto-Iida's formula for the frequency distribution of earthquakes from a deformation-fracture relation. *Jour. Seism. Soc. Japan (Zisin)*, ser. II, vol. 22, p. 136–143.

——— (1969b) Deformation-fracture relation in earthquake genesis and derivation of frequency distribution of earthquakes. *Bull. Earthq. Res. Inst.*, vol. 47, p. 1015–1027.

TSUNEISHI, Y., YOSHIDA, S. and KIMURA, T. (1975) Fault-forming process of the Komyo fault in Central Japan. *Bull. Earthq. Res. Inst.*, vol. 50, p. 415–442.

UTSU, T. (1971) Aftershocks and earthquake statistics (III). *Jour. Fac. Sci., Hokkaido Univ., Ser. VII, Geophysics*, vol. 3, p. 379–441.

小断層の変位の規模別頻度分布とその地殻変形における意義

垣見　俊弘

要　旨

小断層における変位の規模と頻度の関係を，応力状態・断層変位のセンス・媒質のダクティリティ等，断層形成条件の異なる幾つかの場合について検討した．いずれも，落差が T と $T+dT$ の範囲にある断層の数 N は，K, k, m を常数として，およそ $N(T)dT = KT^{-m}dT$，または，$\log N(T) = k-m \log T$ で表される．南関東の新第三紀層に発達する小断層においては，m 値は1.3から2.4まで広範囲に及んでいる．

常数 K または k は，測定面積と，地域の変形度に関係する断層変位密度の関数である．ベキ数 m は断層変位のスペクトル構造の指標であり，実際上は地域の造構条件，すなわち構造の均一性・応力場の安定性・地域変形の鋭どさ等に関連する量である．調査地域から得られた m 値の変動は，造構条件の違いをよく反映しているように思われる．

断層の落差自体は複数回の変位の結果であるから，N と T の関係は変形の進行に応じて時と共に変化している可能性がある．断層運動の初期にあっては，m 値は共役断層系の両セットでともに大きな値を示すであろう．運動がより成熟した段階では，共役両セットのうちどちらか一方が卓越するようになり，その m 値は減少するが，他方の m は以前の段階のままであろう．このように，上記の式で表される断層変位の規模別頻度分布は，造構条件の地域的変化ならびに時間的変化を検討するうえで有効である．

（受付：1979年11月22日；受理：1980年6月10日）